Journal of Materials Chemistry A

PAPER

View Article Online
View Journal | View Issue

Cite this: J. Mater. Chem. A, 2014, 2, 2323

The assembly of dendrimer-stabilized gold nanoparticles onto electrospun polymer nanofibers for catalytic applications†

Dengmai Hu,[a] Yunpeng Huang,[b] Hui Liu,[b] Hong Wang,[b] Shige Wang,[a] Mingwu Shen,[b] Meifang Zhu[a] and Xiangyang Shi*[abc]

Received 2nd October 2013
Accepted 19th November 2013

DOI: 10.1039/c3ta13966b

www.rsc.org/MaterialsA

We report here a facile approach to assembling low generation poly(amidoamine) (PAMAM) dendrimer-stabilized gold nanoparticles (Au DSNPs) onto electrospun polymer nanofibrous mats for catalytic applications. In this study, Au DSNPs formed using amine-terminated generation 2 PAMAM dendrimers as stabilizers were assembled onto electrospun polyacrylic acid (PAA)/polyvinyl alcohol (PVA) nanofibrous mats either through electrostatic interactions or through the covalent 1-ethyl-3-(3-dimethyl-aminopropyl)carbodiimide hydrochloride (EDC) coupling reaction. The assembly of Au DSNPs with a mean diameter of 5.4 nm onto the electrospun nanofibrous mats was characterized *via* different techniques. The catalytic activity of the Au DSNP-assembled nanofibrous mats was evaluated by the transformation of 4-nitrophenol to 4-aminophenol. We show that both approaches enable the efficient assembly of Au DSNPs onto nanofiber surfaces and the as prepared Au DSNP-containing nanofibers formed *via* both approaches have excellent catalytic activity and reusability. However, the Au DSNP-assembled nanofibers *via* electrostatic physical interactions display a much higher catalytic activity than those formed *via* the chemical assembly approach. The facile dendrimer-mediated assembly approach to modifying electrospun nanofibers may be used to fabricate other composite nanofiber systems for applications in catalysis, sensing, and biomedical sciences.

Introduction

Electrospinning is recognized as one of the most powerful technologies to create fibers with diameters ranging from tens of nanometers to several micrometers.[1–4] For improved functionality and applicability, organic/inorganic hybrid nanofibers are generally required to be fabricated.[5–7] The common strategy used to form hybrid nanofibers is to mix the inorganic components with polymer solution for subsequent electrospinning. For instance, nanoclay materials (*e.g.*, halloysite[5,8–11] and laponite[6,12]), hydroxyapatite nanorods,[13,14] and carbon nanotubes,[15–18] have been incorporated within polymer nanofibers for applications in tissue engineering, pharmaceutical sciences, and environmental technology. Hybrid nanofibers can also be formed using preformed electrospun polymer nanofibers as nanoreactors.[18–22] Our previous work has shown that metal nanoparticles (NPs) of Fe,[18,21,22] Au,[19] Pd,[23] Fe/Pd,[20] and Fe/Ni[24] can be immobilized within polyacylic acid (PAA)/polyvinyl alcohol (PVA) or polyethyleneimine (PEI)/PVA nanofibers for environmental or catalytic applications. These hybrid nanofibers share the common features that the active functional groups within the nanofibers (*e.g.*, carboxyl or amine) are able to complex metal ions for the subsequent reductive formation of metal NPs. Furthermore, polymer nanofibers can also be functionalized *via* surface self-assembly, creating metal NP-assembled hybrid nanofibers.[25,26] The major advantage of the metal NP-assembled polymer nanofibers is that the properties or functionalities of metal NPs can be sufficiently employed due to the location of the metal NPs on the surfaces of nanofibers with a high surface area to volume ratio. Therefore, it is crucial to develop versatile technologies to generate metal NP-assembled hybrid nanofibers.

Our previous work has shown that polymer nanofibers can be assembled with polyelectrolyte multilayers for Fe NP immobilization,[27] and polyelectrolyte/carbon nanotube multilayers for enhanced cellular proliferation.[28] For the effective assembly of nanofiber surfaces, the surface of nanofibers and the used polyelectrolytes or inorganic components should possess functional groups, allowing for effective chemical or physical interactions. Therefore, to create metal NP-assembled hybrid nanofibers, it is a prerequisite to prepare functionalized stable metal NPs prior to the self-assembly process.

[a]State Key Laboratory for Modification of Chemical Fibers and Polymer Materials, College of Materials Science and Engineering, Donghua University, Shanghai 201620, P. R. China

[b]College of Chemistry, Chemical Engineering and Biotechnology, Donghua University, Shanghai 201620, P. R. China. E-mail: xshi@dhu.edu.cn

[c]CQM – Centro de Química da Madeira, Universidade da Madeira, Campus da Penteada, 9000-390 Funchal, Portugal

† Electronic supplementary information (ESI) available: Additional experimental results. See DOI: 10.1039/c3ta13966b

Dendrimers are a family of highly branched, monodispersed, synthetic macromolecules with well-defined composition, architecture, and abundant surface functional groups.[29] The uses of dendrimers, especially poly(amidoamine) (PAMAM) dendrimers as powerful stabilizers and templates to generate metal NPs have attracted increasing attention.[30] Dendrimers can be used as templates to form dendrimer-entrapped metal NPs,[31–34] where each metal NP is entrapped within one dendrimer molecule. Dendrimers can also be used as stabilizers to form dendrimer-stabilized metal NPs (metal DSNPs),[35–38] where each metal NP is surrounded by multiple dendrimer molecules. In our previous research,[35] we have shown that amine-terminated generation 2 (G2) PAMAM dendrimers can be adopted as stabilizers to form stable aminated Au DSNPs through a facile hydrothermal approach. In another work, Esumi and his coworkers prepared gold-dendrimer nanocomposites by UV irradiation.[39] Given the advantages of the use of dendrimers to create functionalized metal NPs, it is reasonable to hypothesize that Au DSNPs could be assembled onto the surface of electrospun polymer nanofibers for catalytic applications.

For the catalytic applications of metal NPs with different compositions,[40–43] it is important to maintain the catalytic activity of the particles and simultaneously to make the metal NPs easily recyclable and reusable. Our previous studies have shown that electrospun PEI/PVA nanofibers are able to serve as nanoreactors to immobilize Au[19] or Pd[20] NPs for catalytic applications with good recyclability and reusability. The nanofiber immobilization approach enables the efficient distribution of metal NPs both within the interior and onto the surface of the nanofibers, significantly improving the stability of the metal NPs. Therefore, besides the similar advantages of the metal NP-immobilized nanofibers, it is expected that metal NPs assembled solely on the surface of polymer nanofibers may be more efficient for catalytic applications.

In this present study, aminated Au DSNPs were first formed using amine-terminated G2 PAMAM dendrimers as stabilizers using a hydrothermal approach (Scheme 1a). The formed Au DSNPs were then assembled onto the surface of crosslinked electrospun PAA/PVA nanofibers *via* either physical electrostatic interactions or covalent chemical bonding (Scheme 1b). The formed Au DSNPs and Au DSNP-assembled PAA/PVA were characterized *via* different techniques. Finally the catalytic activity of the formed Au DSNP-assembled nanofibers was assessed by the transformation of 4-nitrophenol to 4-aminophenol. To our knowledge, this is the first report related to the combination of electrospinning and dendrimer nanotechnology to generate metal NP-assembled hybrid nanofibers for catalytic applications.

Experimental section

Materials

Ethylenediamine core amine-terminated G2 PAMAM dendrimers (G2.NH_2) were purchased from Dendritech (Midland, MI, USA). Chloroauric acid ($HAuCl_4$) was from Sinopharm Chemical Reagent Co., Ltd. (China). PAA (average $M_w = 240\,000$, 25% in water) was obtained from Aldrich. PVA (88% hydrolyzed, $M_w = 88\,000$) and 1-ethyl-3-(3-dimethylaminopropyl)carbodiimide hydrochloride (EDC) were acquired from J&K chemical. The water used in all of the experiments was purified using a Milli-Q Plus 185 water purification system (Millipore, Bedford, MA, USA) with a resistivity higher than 18 MΩ cm. All other chemicals were of analytical grade.

Synthesis of Au DSNPs

Au DSNPs were prepared using G2.NH_2 dendrimers as stabilizers through a hydrothermal method according to our previous work (Scheme 1a).[36] In brief, an aqueous G2.NH_2 dendrimer solution (10 mg mL^{-1}, 15 mL) was preheated in a 60 °C water bath for 30 min. Then, $HAuCl_4$ (30 mg mL^{-1}, 1.895 mL) was added into the G2.NH_2 dendrimer solution with the Au salt–dendrimer molar ratio of 3 : 1. The reaction was maintained at 60 °C for 3 h under magnetic stirring. With the solution color gradually changing from yellow to red, Au NPs were formed. After that, the mixture was cooled down to room temperature, dialyzed against water (6 times, 2 L) for 2 days to remove the excess reactants, followed by lyophilization to get the $\{(Au^0)_3$-G2.$NH_2\}$ DSNPs (Au DSNPs).

Preparation of the crosslinked PAA/PVA nanofibrous mats

The procedure to fabricate the crosslinked electrospun PAA/PVA nanofibrous mats was adopted from our previous work.[20] Briefly, a PVA/PAA homogeneous solution with a PVA/PAA mass ratio of 1 : 1 and a total polymer concentration of 12% was prepared before electrospinning. The electrospinning was carried out at ambient temperature using a syringe with a needle having an inner diameter of 0.8 mm at an applied voltage of 16.8 kV. The feeding rate and the tip-to-collector distance were set to be 0.5 mL h^{-1} and 25 cm, respectively. The freshly prepared PAA/PVA nanofibrous mats were crosslinked upon a heating treatment at 145 °C for 30 min to render them water stable according to the literature.[20]

Preparation of the Au DSNP-assembled PAA/PVA nanofibrous mats

The process to physically assemble the Au DSNPs onto the PAA/PVA nanofibrous mats is shown in Scheme 1b. In brief, a crosslinked nanofibrous mat (1 × 2 cm^2, 5 mg) was dipped into water (0.8 mL) for 3 h to allow the available free PAA carboxyl groups to be deprotonated. Then, the Au DSNP aqueous solution (2.6 mM, 0.2 mL) was added onto the nanofibrous mat and the liquid was left on the mat surface for 20 min to allow the electrostatic deposition of the aminated Au DSNPs, followed by rinsing with water for 3 times to remove excess Au DSNPs. The formed Au DSNP-assembled nanofibrous mats were dried under vacuum at room temperature for 24 h, and stored in a desiccator before use.

Au DSNPs were also covalently assembled onto the PAA/PVA nanofibrous mats through a chemical reaction between the amino groups of the G2.NH_2 dendrimers and the available free carboxyl groups of PAA (Scheme 1b). Differently from the physical assembly process, EDC was employed here to activate

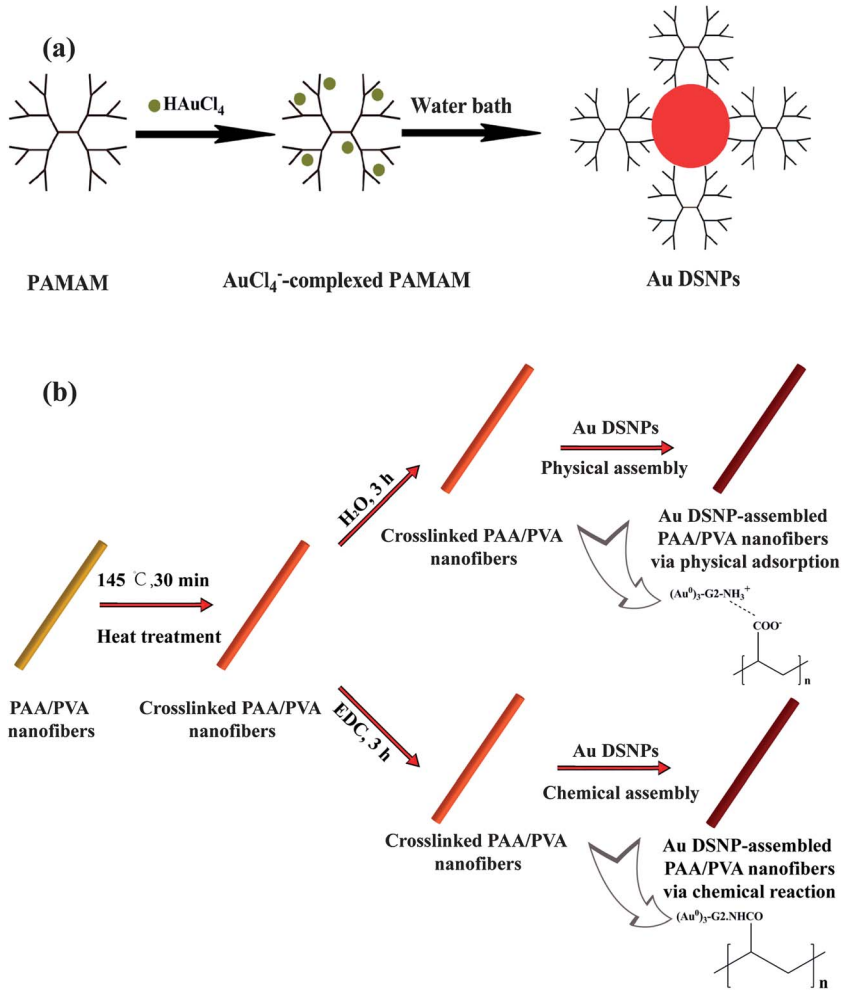

Scheme 1 Schematic illustration of the synthesis process of Au DSNPs (a) and the assembly of Au DSNPs onto electrospun PAA/PVA nanofibers through physical adsorption and chemical reaction (b).

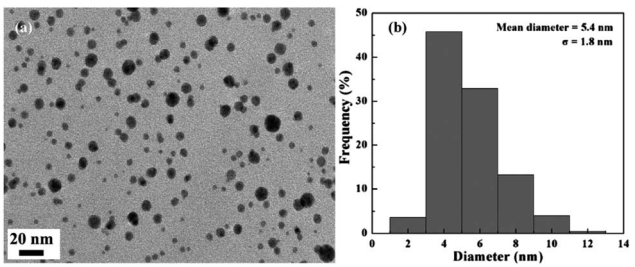

Fig. 1 TEM image (a) and size distribution histogram (b) of the formed Au DSNPs.

the free PAA carboxyl groups to react with the dendrimer amines. In a typical procedure, a crosslinked nanofibrous mat (1×2 cm^2, 5 mg) was dipped into an EDC aqueous solution (32.6 M, 0.8 mL) under constant vibration using a shaker at room temperature for 3 h, followed by adding the Au DSNPs aqueous solution (2.6 mM, 0.2 mL) under vibration. The nanofibrous mat was taken out after 2 days, rinsed with water 3 times, dried under vacuum at room temperature for 24 h, and finally stored in a desiccator before use.

Characterization techniques

The morphology of the electrospun PAA/PVA nanofibrous mats before and after Au DSNP assembly was observed using scanning electron microscopy (SEM, TM-100, Hitachi, Japan) with an operating voltage of 10 kV. Prior to the SEM measurements, samples were sputter-coated with 10 nm thick carbon films. The elemental composition of the samples was analyzed by energy dispersive spectroscopy (EDS, IE300X, Oxford, U.K.) attached to the SEM. UV-vis spectrometry (Lambda 950 UV-vis spectrometer) was also used to characterize the assembly of the Au DSNPs onto the PVA/PAA nanofibrous mats *via* the measurement of reflectance induced by the Au DSNPs. The samples were fixed onto glass slides before the measurements. To observe the distribution of Au DSNPs onto the nanofibers, the Au DSNP-assembled polymer nanofibrous mats were embedded in epoxy resin and cut into ultrathin sections with an ultramicrotome equipped with a diamond knife. Transmission electron microscopy (TEM, JEM2100, JEOL Ltd., Japan) was performed at an operating voltage of 200 kV. The diameters of the nanofibers and particle sizes were measured using image analysis software ImageJ 1.40G (http://

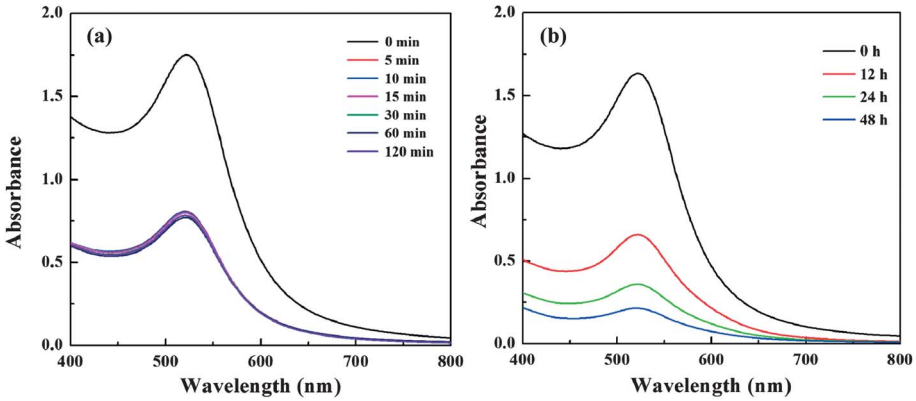

Fig. 2 UV-vis spectra of the Au DSNP solution after physical (a) and chemical (b) assembly onto the surface of the nanofibers at different time points.

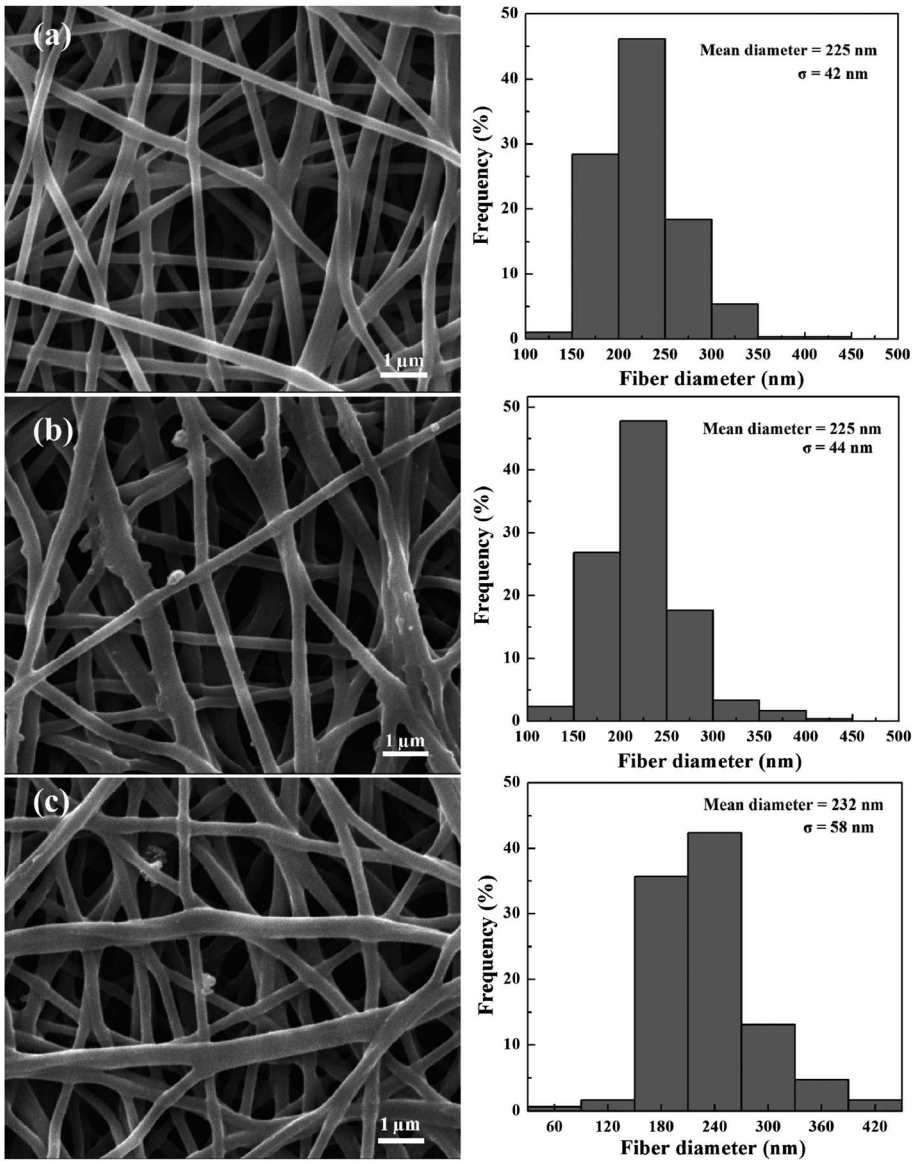

Fig. 3 SEM images and diameter distribution histograms of PAA/PVA nanofibers without Au DSNPs (a), and Au DSNP-assembled PAA/PVA nanofibers formed *via* physical adsorption (b), Au DSNP-assembled PAA/PVA nanofibers formed *via* chemical reaction (c).

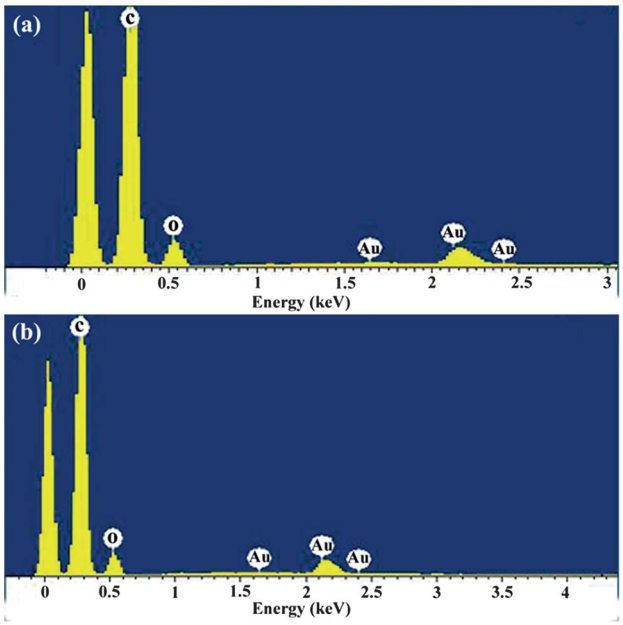

Fig. 4 EDS spectra of the Au DSNP-assembled PAA/PVA nanofibers formed *via* physical adsorption (a) and chemical reaction (b).

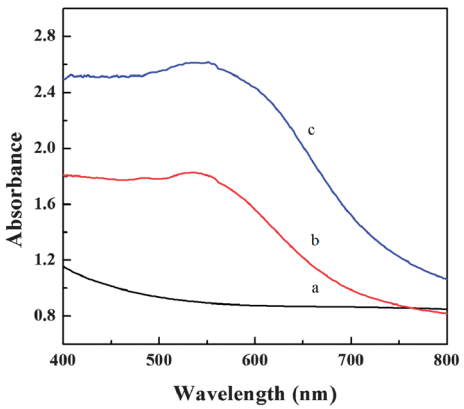

Fig. 5 Reflectance UV-vis spectra of PAA/PVA fibers without Au DSNPs (a), Au DSNP-assembled PAA/PVA nanofibers formed *via* physical adsorption (b), and Au DSNP-assembled PAA/PVA nanofibers formed *via* chemical reaction (c).

rsb.info.nih.gov/ij/download.html). At least 300 randomly selected nanofibers or NPs in different SEM or TEM images were analyzed for each sample to acquire the diameter/size distribution histograms. Thermal gravimetric analysis (TGA) was carried out using a TG 209 F1 (NETZSCH Instruments Co., Ltd., Germany) thermogravimetric analyzer with a heating rate of 10 °C min^{-1} in air. To determine the Au content in the Au DSNP-assembled PAA/PVA nanofibrous mats before and after catalytic reactions, a Leeman Prodigy inductively coupled plasma-optical emission spectroscopy (ICP-OES) system (Hudson, NH03051, USA) was used. The Au DSNP assembled fibrous mat (5 mg) was treated with aqua regia (500 μL) for 3 h. The extract solution was diluted before analysis.

Catalysis experiments

A model reaction to transform 4-nitrophenol to 4-aminophenol was selected to evaluate the catalytic efficiency and reusability of the Au DSNP-assembled PAA/PVA nanofibrous mats formed *via* either the physical or chemical assembly process according to the procedure reported in the literature.[19] In brief, a solution mixture containing 4-nitrophenol (0.6 mL, 10 mM), $NaBH_4$ aqueous solution (0.6 mL, 10 M), and water (16.8 mL) was prepared in a 25 mL beaker. Then, an Au DSNP-assembled free-standing nanofibrous mat with an Au amount of 0.5 mg was immersed into the above mixture solution at room temperature, followed by gentle magnetic stirring. At a given time interval, 0.5 mL of the aqueous solution was withdrawn and diluted to 1.0 mL for the detection of the transformation efficiency using a Lambda-25 UV-vis spectrometer (Perkin-Elmer, USA). To verify the reusability of the Au DSNP-assembled PAA/PVA nanofibrous mat, the mat was washed with water and blotted with filter paper before it was reused for the next cycle of catalytic reaction. For comparison, the cross-linked free-standing PAA/PVA nanofibrous mats without the assembly of Au DSNPs were also tested. The transformation efficiency of 4-nitrophenol to 4-aminophenol was calculated according to the following equation:

$$\text{remaining fraction of 4-nitrophenol} = C_t/C_0 \times 100\% \quad (1)$$

where C_0 and C_t are the initial concentration of 4-nitrophenol and 4-nitrophenol concentration at a given time interval, respectively.

Results and discussion

Preparation and characterization of Au DSNP-assembled PAA/PVA nanofibrous mats

To construct Au DSNP-assembled PAA/PVA nanofibrous mats, Au DSNPs were first synthesized using G2 dendrimers as stabilizers according to the protocol described in our previous reports.[35,36] TEM was used to characterize the formed $\{(Au^0)_3$-G2.$NH_2\}$ DSNPs (Fig. 1a). It can be seen that the formed Au DSNPs are spherical in shape with a mean diameter of 5.4 ± 1.8 nm (Fig. 1b), in agreement with our previous reports.[35,36]

Similar to our previous work,[18,21,22] PAA/PVA nanofibrous mats were rendered water stable by crosslinking before being used in an aqueous environment. The PAA/PVA nanofibers were crosslinked by a heating treatment at 145 °C for 30 min, which makes the carboxyl groups of PAA react with the hydroxyl groups of PVA to form ester bonds. Then, the aminated Au DSNPs were assembled onto the nanofiber surfaces *via* both physical and chemical approaches.

UV-vis spectroscopy was performed to monitor the assembly process (Fig. 2). The surface plasmon resonance (SPR) band located at 525 nm for the Au DSNP solution dramatically decreased after 5 min physical adsorption and remained almost unchanged until 120 min (Fig. 2a). This indicates that the Au DSNPs are able to be quickly adsorbed onto the fibrous mat *via* electrostatic assembly. In contrast, the chemical assembly involves an EDC-mediated coupling of the PAA carboxyl groups

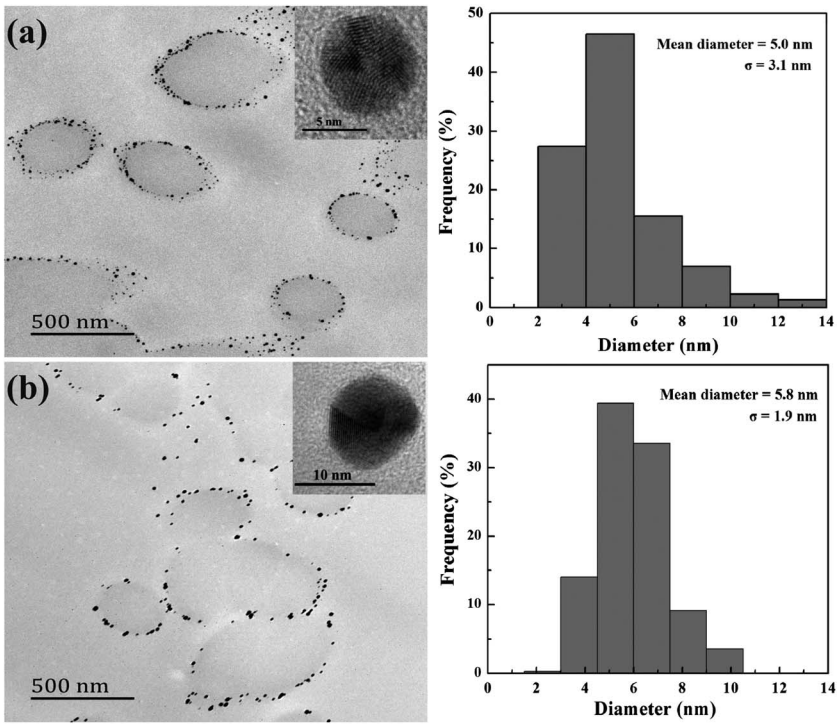

Fig. 6 TEM images and size distribution histograms of the Au DSNPs assembled onto PAA/PVA nanofibers *via* physical adsorption (a) and chemical reaction (b). The insets show the high-resolution TEM images of the respective Au DSNPs.

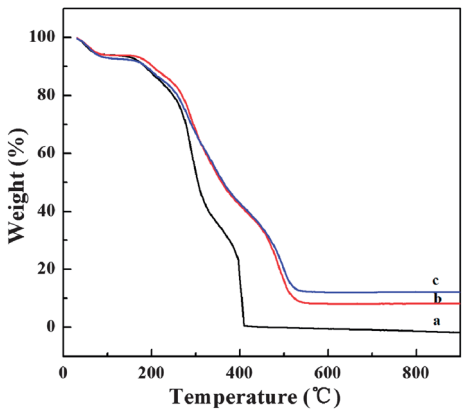

Fig. 7 TGA curves of the PAA/PVA nanofibers before (Curve a) and after assembly with the Au DSNPs *via* physical adsorption (Curve b) and chemical reaction (Curve c).

and the amines of the Au DSNPs. This process was quite slow, and the SPR peak at 525 nm for the Au DSNP solution continuously decreased with the time of reaction and reached its lowest point at 48 h in the studied time period (Fig. 2b).

SEM was performed to observe the morphology of the formed nanofibrous mats before and after the assembly of Au DSNPs (Fig. 3). Similar to our previous work,[22] crosslinked PAA/PVA nanofibers with a smooth and uniform morphology and random orientation were generated with a mean diameter of 225 ± 42 nm (Fig. 3a). The physical assembly of the Au DSNPs does not seem to alter the morphology of the PAA/PVA nanofibers and the fiber diameter (Fig. 3b). Similarly, the chemical assembly of the Au DSNPs does not alter the smooth morphology of the PAA/PVA nanofibers (Fig. 3c), but leads to a slight increase of the fiber diameter (232 ± 58 nm). The increased fiber diameter should be caused by the swelling of the nanofibers that are treated by EDC for the chemical assembly of Au DSNPs in a relatively long time period when compared with the physical assembly process. The assembly of Au DSNPs onto the surface of nanofibers was further confirmed by EDS analysis of the elemental composition of the nanofibers (Fig. 4). Au element can be clearly seen in the EDS spectrum of the Au DSNP-assembled nanofibrous mats prepared by both physical adsorption (Fig. 4a) and chemical reaction (Fig. 4b). The elemental oxygen observed in both cases could be attributed to the hydroxyl group of the PVA and the carboxyl group of the PAA in the nanofibers.

Reflectance UV-vis spectroscopy was also used to confirm the assembly of Au DSNPs (Fig. 5). In contrast to the PAA/PVA nanofibers without the assembly of Au DSNPs that do not display apparent absorption features, the Au DSNP-assembled PAA/PVA nanofibers prepared by both physical adsorption and chemical assembly show the typical SPR peak at 538 nm associated with the assembled Au DSNPs. This further demonstrated the successful assembly of Au DSNPs onto the surface of PAA/PVA nanofibers.[25]

The distribution of Au DSNPs onto the surface of PAA/PVA nanofibers was characterized by cross-sectional TEM imaging of the hybrid nanofibers (Fig. 6). Round-shaped patterns of the Au DSNPs are clearly observed, indicating that Au DSNPs were successfully assembled along the cross section of the fibers (Fig. 6a and b). The mean diameter of the Au DSNPs assembled

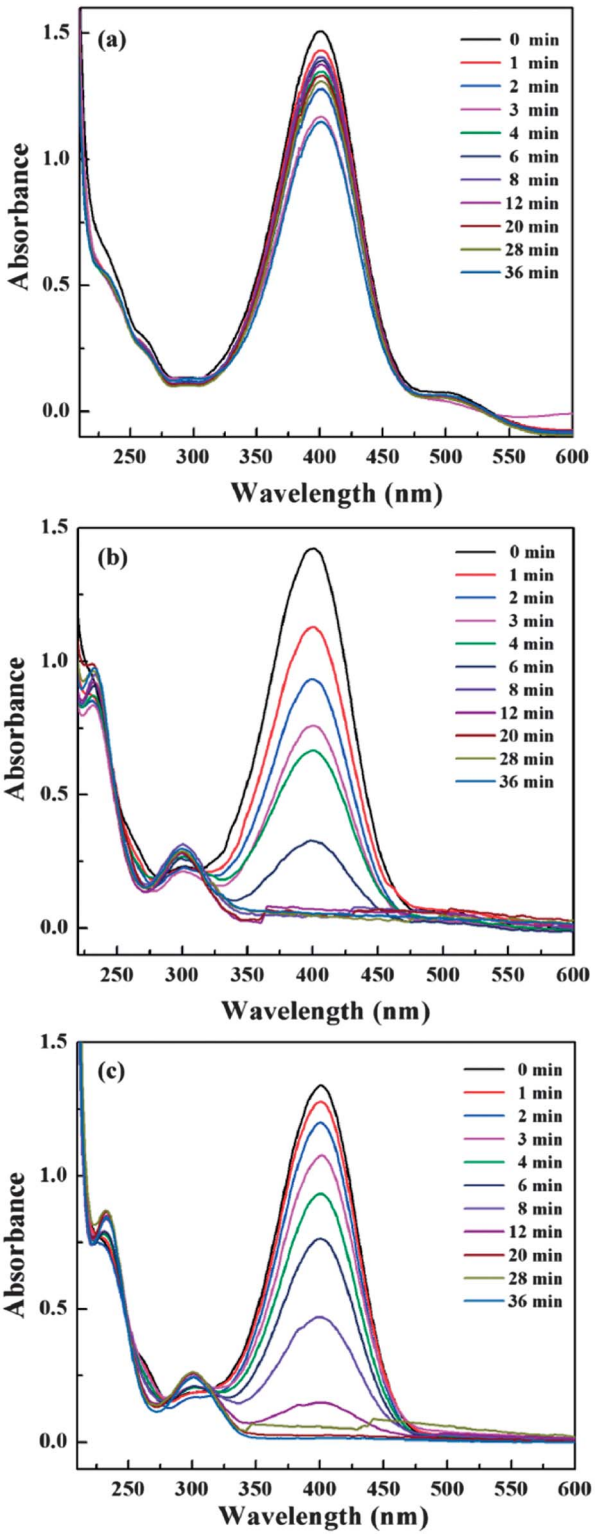

Fig. 8 UV-vis spectra of the 4-nitrophenol aqueous solution treated with nanofibers at different time intervals: PAA/PVA nanofibers without Au DSNPs (a), Au DSNP-assembled PAA/PVA nanofibers formed *via* physical adsorption (b), and Au DSNP-assembled PAA/PVA nanofibers formed *via* chemical reaction (c).

by physical adsorption was estimated to be 5.0 ± 3.1 nm, while the mean diameter of the Au DSNPs assembled by chemical reaction was estimated to be 5.8 ± 1.9 nm. The slightly larger size of the Au DSNPs assembled *via* chemical reaction may be due to the longer assembly time, favoring further Ostwald ripening. Differently from our previous study related to the uniform distribution of Au NPs within the entire fiber cross-section of the PEI/PVA nanofibers,[19] the Au DSNPs assembled in this work are solely distributed at the outer shell of the fibers, confirming the success of the assembly *via* both physical and chemical approaches. Furthermore, the crystalline lattice structure of the assembled Au DSNPs can be clearly observed by high-resolution TEM images (Fig. 6, insets).

TGA was used to analyze the composition of the Au DSNP-assembled PAA/PVA nanofibers (Fig. 7). The initial slight weight loss for all the nanofibers should be due to the loss of moisture in the fibers. The major weight loss of the Au DSNP-assembled nanofibrous mats in the region of 170–500 °C is attributed to the decomposition of the PAA/PVA polymers and dendrimers. By comparing the Au DSNP-assembled nanofibrous mats with the Au DSNP-free mats (Fig. 7, Curve a), the assembled Au component onto the nanofibrous mats was estimated to be 8.1% for the physical assembly approach (Fig. 7, Curve b) and 12.0% for the chemical assembly approach (Fig. 7, Curve c), respectively. The higher loading of Au DSNPs *via* the chemical assembly approach (also in line with the above UV-vis spectroscopic data) may be ascribed to the more efficient interaction between the aminated Au DSNPs and the PAA carboxyl groups *via* an EDC-mediated coupling reaction. In contrast, the physical assembly of Au DSNPs onto the fiber surface *via* electrostatic interaction is not strong enough and the interparticle repulsion may lead to a reduced density of the particle coating on the fiber surface.

Catalytic transformation of 4-nitrophenol to 4-aminophenol

We next explored the potential catalytic applications of the Au DSNP-assembled PAA/PVA nanofibrous mats by a model reaction to transform 4-nitrophenol to 4-aminophenol in the presence of $NaBH_4$. It is well-known that the reaction does not proceed without a catalyst.[44] UV-vis spectroscopy was used to monitor the transformation process after the addition of the hybrid nanofibrous mat as a catalyst. Firstly, we selected the Au DSNP-assembled nanofibrous mats formed through physical adsorption as a catalyst. We show that the Au DSNP-assembled nanofibrous mats are able to effectively catalyze the reaction to transform 4-nitrophenol to 4-aminophenol in the presence of $NaBH_4$, similar to our previous work.[19] It is clear that the yellow color of the 4-nitrophenol solution gradually faded with the reaction time (Fig. S1b, ESI†), and the intensity of the characteristic absorption peak of 4-nitrophenol at 400 nm gradually decreased and disappeared within the time frame of 8 min (Fig. 8b). With the decrease of the characteristic absorption peak of 4-nitrophenol, a new characteristic absorption peak of 4-aminophenol started to appear at 300 nm. In contrast, when the PAA/PVA nanofibers without Au DSNPs were exposed to the same reaction mixture, a slight decrease in the intensity of the

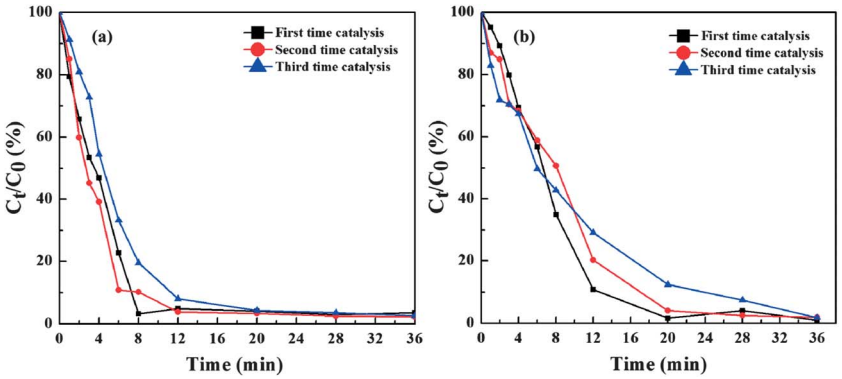

Fig. 9 The remaining fraction of 4-nitrophenol as a function of time for the first, second, and third catalytic transformation reaction cycle: (a) Au DSNP-assembled PAA/PVA nanofibers formed *via* physical adsorption, (b) Au DSNP-assembled PAA/PVA nanofibers formed *via* chemical reaction.

absorption peak at 400 nm was observed within 36 min, which should be associated with the physical adsorption of the 4-nitrophenol onto the surface of the PAA/PVA nanofibrous mats (Fig. 8a and S1a†). This further supports that the superior catalytic transformation of 4-nitrophenol to 4-aminophenol is closely related to the excellent catalytic property of the assembled Au DSNPs.

For comparison, the catalytic properties of the Au DSNP-assembled hybrid mats through chemical reaction were also investigated under similar experimental conditions. We show that with a similar amount of Au content, the Au DSNP-assembled nanofibers formed *via* chemical reaction are also able to catalyze the transformation of 4-nitrophenol to 4-aminophenol (Fig. 8c and S1c†). However, the catalytic efficacy is lower than that of the hybrid mats formed *via* physical assembly. After 20 min, the characteristic absorption peak of 4-nitrophenol at 400 nm disappeared. The relatively low catalytic activity of Au DSNP-assembled PAA/PVA nanofibers formed *via* chemical assembly may be due to the dense packing of the Au DSNPs onto the fiber surfaces, limiting the accessibility of the 4-nitrophenol molecules to undertake the transformation reaction.

For practical catalytic applications, the developed catalyst must have good reusability and recyclability. Although the prepared colloidal gold-dendrimer nanocomposites reported in the literature[39] are able to catalyze the conversion of 4-nitrophenol to 4-aminophenol with a catalytic activity comparable to the Au DSNPs assembled onto the nanofibers in our work, the colloidal gold-dendrimer nanocomposites are difficult to be recycled for further use. The catalytic activity of the Au DSNP-assembled nanofibrous mats was also demonstrated by plotting the remaining fraction of 4-nitrophenol as a function of the exposure time (Fig. 9). After catalyzing the 4-nitrophenol solution for the first time, the hybrid nanofibrous mats were washed with water and blotted by a filter paper before it was reused for the next cycle of catalytic reaction. It can be seen that more than 97% 4-nitrophenol is able to be transformed to 4-aminophenol after 8, 12, and 20 min exposure of the Au DSNP-assembled fiber mats formed *via* physical assembly for the 1st, 2nd, and 3rd reaction cycles, respectively, confirming their reusability (Fig. 9a). In the case of Au DSNP-assembled fiber mats formed *via* chemical assembly, 99% 4-nitrophenol is able to be transformed to 4-aminophenol after 20, 28, and 36 min for the 1st, 2nd, and 3rd reaction cycles, respectively, revealing their good reusability (Fig. 9b). The slightly decreased catalytic activity of both types of Au DSNP-assembled nanofibers with the number of reaction cycles may be due to the fact that the swelling of nanofibers during the multiple catalytic reactions in aqueous solution may introduce more fiber junctions, thereby limiting the accessibility of the reactants to the surface of the Au DSNPs. Taken together, our results illustrate that the as-prepared hybrid nanofibers *via* both the physical and chemical approaches are promising catalysts with high efficiency and reusability. The Au DSNP-assembled nanofibers formed *via* the physical approach display a better catalytic efficiency than those formed *via* the chemical approach. It should be noted that the Au DSNP-assembled hybrid nanofibers formed *via* both physical and chemical approaches display much better catalytic efficiency than the AuNP-immobilized PEI/PVA nanofibers reported in our previous work.[19] This well demonstrates our hypothesis that Au NPs assembled onto fiber surfaces allow for efficient access to the substrate molecules, favoring enhanced catalytic reactions. In contrast, the Au NPs immobilized within the interior of the nanofibers are likely to be insufficiently accessed by substrate molecules for efficient catalytic reactions. Finally, the developed Au DSNP-assembled fiber mats formed *via* either the physical assembly or chemical reaction were demonstrated to be quite stable, and the fibrous morphology could be maintained after 3 times of catalytic use (Fig. S2, ESI†). In addition, the Au NPs did not seem to have an appreciable release into the reaction medium, which was confirmed by the EDS analysis of both Au DSNP-assembled nanofibers after 3 catalytic reaction cycles (Fig. S3, ESI†). Further ICP-OES analysis showed that the Au content for the Au DSNPs-assembled nanofibers *via* physical assembly changed from 8.3% to 7.6% after 3 cycles of catalytic reactions. Similarly, the 3 cycles of catalytic reaction did not seem to change the Au content significantly for the Au DSNP-assembled fibrous mat *via* chemical assembly (from 10.0% to 9.5%).

Conclusions

In summary, we have developed a novel approach to assembling Au DSNPs onto eletrospun polymer nanofibrous mats for catalytic applications. The dendrimer stabilization approach enables the generation of aminated Au DSNPs with a mean diameter of 5.4 nm that can be assembled onto electrospun PAA/PVA nanofibrous mats through either physical absorption or chemical reaction. Although the loading of Au DSNPs *via* chemical reaction is more efficient than that *via* physical assembly, the catalytic activity of the Au DSNP-assembled nanofibers *via* the physical assembly is demonstrated to be higher in the transformation of 4-nitrophenol to 4-aminophenol than that of the hybrid fibers formed *via* the chemical approach. Moreover, the Au DSNP-assembled hybrid nanofibers formed *via* both approaches display good reusability. The approach to assembling Au DSNPs onto nanofibers may be extended to prepare other metal NP-assembled hybrid nanofibers for applications in catalysis, sensing, and biomedical sciences.

Acknowledgements

This research was financially supported by the Program for New Century Excellent Talents in University, State Education Ministry, the High-Tech Research and Development Program of China (2012AA030309), and the Fund of the Science and Technology Commission of Shanghai Municipality (12520705500 for M. S.). X.S. gratefully acknowledges the Fundaçao para a Ciência e a Tecnologia (FCT) and Santander bank for the Chair in Nanotechnology, and the FCT through the Strategic Plan PEst-OE/QUI/UI0674/2011. M.Z. thanks the National Natural Science Foundation of China (50925312) for support.

Notes and references

1 Q. P. Pham, U. Sharma and A. G. Mikos, *Nano Lett.*, 2006, **12**, 1197–1211.
2 M. M. Demir, M. A. Gulgun, Y. Z. Menceloglu, B. Erman, S. S. Abramchuk, E. E. Makhaeva, A. R. Khokhlov, V. G. Matveeva and M. G. Sulman, *Macromolecules*, 2004, **37**, 1787–1792.
3 K. Yoon, B. S. Hsiao and B. Chu, *J. Mater. Chem.*, 2008, **18**, 5326–5334.
4 S. K. Chae, H. Park, J. Yoon, C. H. Lee, D. J. Ahn and J. M. Kim, *Adv. Mater.*, 2007, **19**, 521–524.
5 R. Qi, X. Cao, M. Shen, R. Guo, J. Yu and X. Shi, *J. Biomater. Sci., Polym. Ed.*, 2012, **23**, 299–313.
6 S. Wang, R. Castro, X. An, C. Song, Y. Luo, M. Shen, H. Tomás, M. Zhu and X. Shi, *J. Mater. Chem.*, 2012, **22**, 23357–23367.
7 S. Wang, Y. Zhao, M. Shen and X. Shi, *Ther. Delivery*, 2012, **3**, 1155–1169.
8 R. Qi, R. Guo, M. Shen, X. Cao, L. Zhang, J. Xu, J. Yu and X. Shi, *J. Mater. Chem.*, 2010, **20**, 10622–10629.
9 R. Qi, R. Guo, F. Zheng, H. Liu, J. Yu and X. Shi, *Colloids Surf., B*, 2013, **110**, 148–155.
10 R. Qi, M. Shen, X. Cao, R. Guo, X. Tian, J. Yu and X. Shi, *Analyst*, 2011, **136**, 2897–2903.
11 Y. Zhao, S. Wang, Q. Guo, M. Shen and X. Shi, *J. Appl. Polym. Sci.*, 2013, **127**, 4825–4832.
12 S. Wang, F. Zheng, Y. Huang, Y. Fang, M. Shen, M. Zhu and X. Shi, *ACS Appl. Mater. Interfaces*, 2012, **4**, 6393–6401.
13 F. Zheng, S. Wang, M. Shen, M. Zhu and X. Shi, *Polym. Chem.*, 2013, **4**, 933–941.
14 F. Zheng, S. Wang, S. Wen, M. Shen, M. Zhu and X. Shi, *Biomaterials*, 2013, **34**, 1402–1412.
15 H. Liao, R. Qi, M. Shen, X. Cao, R. Guo, Y. Zhang and X. Shi, *Colloids Surf., B*, 2011, **84**, 528–535.
16 F. Liu, R. Guo, M. Shen, X. Cao, X. Mo, S. Wang and X. Shi, *Soft Mater.*, 2010, **8**, 239–253.
17 F. Liu, R. Guo, M. Shen, S. Wang and X. Shi, *Macromol. Mater. Eng.*, 2009, **294**, 666–672.
18 S. Xiao, M. Shen, R. Guo, Q. Huang, S. Wang and X. Shi, *J. Mater. Chem.*, 2010, **20**, 5700–5708.
19 X. Fang, H. Ma, S. Xiao, M. Shen, R. Guo, X. Cao and X. Shi, *J. Mater. Chem.*, 2011, **21**, 4493–4501.
20 Y. Huang, H. Ma, S. Wang, M. Shen, R. Guo, X. Cao, M. Zhu and X. Shi, *ACS Appl. Mater. Interfaces*, 2012, **4**, 3054–3061.
21 S. Xiao, H. Ma, M. Shen, S. Wang, Q. Huang and X. Shi, *Colloids Surf., A*, 2011, **381**, 48–54.
22 S. Xiao, M. Shen, R. Guo, S. Wang and X. Shi, *J. Phys. Chem. C*, 2009, **113**, 18062–18068.
23 H. Ma, Y. Huang, M. Shen, R. Guo, X. Cao and X. Shi, *J. Hazard. Mater.*, 2012, **211**, 349–356.
24 H. Ma, Y. Huang, M. Shen, D. Hu, H. Yang, M. Zhu, S. Yang and X. Shi, *RSC Adv.*, 2013, **3**, 6455–6465.
25 H. Dong, E. Fey, A. Gandelman and W. E. Jones, *Chem. Mater.*, 2006, **18**, 2008–2011.
26 H. Dong, D. Wang, G. Sun and J. P. Hinestroza, *Chem. Mater.*, 2008, **20**, 6627–6632.
27 S. Xiao, S. Wu, M. Shen, R. Guo, Q. Huang, S. Wang and X. Shi, *ACS Appl. Mater. Interfaces*, 2009, **1**, 2848–2855.
28 Y. Luo, S. Wang, M. Shen, R. Qi, Y. Fang, R. Guo, H. Cai, X. Cao, H. Tomas, M. Zhu and X. Shi, *Carbohydr. Polym.*, 2013, **91**, 419–427.
29 D. A. Tomalia and J. M. Fréchet, *J. Polym. Sci., Part A: Polym. Chem.*, 2002, **40**, 2719–2728.
30 M. Shen and X. Shi, *Nanoscale*, 2010, **2**, 1027–1032.
31 X. Shi, S. H. Wang, S. Meshinchi, M. E. Van Antwerp, X. Bi, I. Lee and J. R. Baker, Jr, *Small*, 2007, **3**, 1245–1252.
32 X. Shi, S. H. Wang, H. Sun and J. R. Baker, Jr, *Soft Matter*, 2007, **3**, 71–74.
33 X. Y. Shi, I. H. Lee and J. R. Baker, Jr, *J. Mater. Chem.*, 2008, **18**, 586–593.
34 R. Shukla, E. Hill, X. Shi, J. Kim, M. C. Muniz, K. Sun and J. R. Baker, Jr, *Soft Matter*, 2008, **4**, 2160–2163.
35 H. Liu, Y. Xu, S. Wen, Q. Chen, L. Zheng, M. Shen, J. Zhao, G. Zhang and X. Shi, *Chem.–Eur. J.*, 2013, **19**, 6409–6416.
36 H. Liu, Y. Xu, S. Wen, J. Zhu, L. Zheng, M. Shen, J. Zhao, G. Zhang and X. Shi, *Polym. Chem.*, 2013, **4**, 1788–1795.

37 X. Shi, K. Sun and J. R. Baker, Jr, *J. Phys. Chem. C*, 2008, **112**, 8251–8258.
38 X. Shi, S. H. Wang, M. E. Van Antwerp, X. Chen and J. R. Baker, Jr, *Analyst*, 2009, **134**, 1373–1379.
39 K. Hayakawa, T. Yoshimura and K. Esumi, *Langmuir*, 2003, **19**, 5517–5521.
40 W. Niu, S. Zheng, D. Wang, X. Liu, H. Li, S. Han, J. Chen, Z. Tang and G. Xu, *J. Am. Chem. Soc.*, 2008, **131**, 697–703.
41 J. Wang, J. Gong, Y. Xiong, J. Yang, Y. Gao, Y. Liu, X. Lu and Z. Tang, *Chem. Commun.*, 2011, **47**, 6894–6896.
42 J. Gong, F. Zhou, Z. Li and Z. Tang, *Langmuir*, 2012, **28**, 8959–8964.
43 J. Qi, J. Chen, G. Li, S. Li, Y. Gao and Z. Tang, *Energy Environ. Sci.*, 2012, **5**, 8937–8941.
44 H. Jiang, T. Akita, T. Ishida, M. Haruta and Q. Xu, *J. Am. Chem. Soc.*, 2011, **133**, 1304–1306.